AGU PUBLICATIONS

Geophysical Research Letters

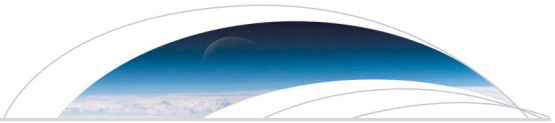

RESEARCH LETTER
10.1002/2013GL058773

Key Points:
- High terrestrial ecosystem emissions of trace gas and aerosol precursors in Pliocene
- Tropospheric ozone and aerosols have large impact on Pliocene radiation budget
- Discover new vegetation-mediated ozone and aerosol slow climate feedback

Supporting Information:
- Readme
- Figure S1a
- Figure S1b
- Figure S2a
- Figure S2b
- Figure S2c
- Figure S2d
- Figure S3
- Figure S4
- Table S1
- Table S2

Correspondence to:
N. Unger,
nadine.unger@yale.edu

Citation:
Unger, N., and X. Yue (2014), Strong chemistry-climate feedback in the Pliocene, *Geophys. Res. Lett.*, *41*, 527–533, doi:10.1002/2013GL058773.

Received 23 NOV 2013
Accepted 20 DEC 2013
Accepted article online 23 DEC 2013
Published online 17 JAN 2014

Strong chemistry-climate feedbacks in the Pliocene

Nadine Unger[1] and Xu Yue[1]

[1]School of Forestry and Environmental Studies, Yale University, New Haven, Connecticut, USA

Abstract The Pliocene epoch was the last sustained interval when global climate was significantly warmer than today but has been difficult to explain fully based on the external forcings from atmospheric carbon dioxide and surface albedo. Here we use an Earth system model to simulate terrestrial ecosystem emissions and atmospheric chemical composition in the mid-Pliocene (about 3 million years ago) and the preindustrial (~1750s). Tropospheric ozone and aerosol precursors from vegetation and wildfire are ~50% and ~100% higher in the mid-Pliocene due to the spread of the tropical savanna and deciduous biomes. The chemistry-climate feedbacks contribute a net global warming that is +30–250% of the carbon dioxide effect and a net aerosol global cooling that masks 15–100% of the carbon dioxide effect. These large vegetation-mediated ozone and aerosol feedbacks operate on centennial to millennial timescales in the climate system and have not previously been included in paleoclimate sensitivity assessments.

1. Introduction

The middle Pliocene warm period (mid-Pliocene) about 3 million years ago (Ma) has been extensively examined as an analog of possible future planetary conditions in response to anthropogenic climate change [*Haywood et al.*, 2010]. Ostensibly, this deep-time period appears to be an ideal test bed to understand the future greenhouse world because the external forcings that control the global climate, atmospheric carbon dioxide (CO_2) and global geography, were almost identical to the modern climate state. Yet the mid-Pliocene climate was rather different than today for reasons that are not well understood. Earth's global average surface air temperature (SAT) was 2–3°C warmer than the preindustrial (~1750s), and meridional and zonal temperature gradients were substantially reduced even though maximum ocean temperatures were similar to the preindustrial [*Ballantyne et al.*, 2010; *Dowsett et al.*, 2010; *Robinson*, 2009]. These structural climate differences, which were even more pronounced earlier in the Pliocene [*Fedorov et al.*, 2013], are difficult to explain based on the known external forcings. Current generation coupled ocean-atmosphere global climate models are not able to reproduce fully the mid-Pliocene proxy data [*Dowsett et al.*, 2012; *Haywood and Valdes*, 2004; *Lunt et al.*, 2010], which suggests that other climate forcing mechanisms may play a role in the Pliocene climate.

The rapidly reacting, radiatively active compounds, tropospheric ozone (O_3), and aerosols, are fundamental components of Earth's global climate system. O_3 is a greenhouse gas that warms the atmosphere. Aerosols have complex direct effects on climate involving both warming and cooling mechanisms. Primary organic matter, biogenic secondary organic aerosol (BSOA), and secondary inorganic aerosols, such as nitrate and sulfate, scatter solar radiation back to space and lead to cooling. Black carbon (soot) absorbs solar radiation and warms the atmosphere. Aerosols impose further indirect effects on climate by modifying the properties of clouds. Natural emissions from terrestrial ecosystems are major sources of trace gas and particle precursors that regulate the formation and global budgets of O_3 and aerosols [*Arneth et al.*, 2010a; *Carslaw et al.*, 2010]. Vegetation emits vast quantities of biogenic volatile organic compounds (BVOCs), mostly as isoprene and monoterpenes, which are important precursors for O_3 and BSOA [*Guenther et al.*, 2012]. Wildfire is a major source of black carbon and primary organic matter [*van der Werf et al.*, 2010]. In addition, wildfire emits a host of other short-lived gases, including carbon monoxide (CO), nitrogen oxides ($NO_x \equiv NO + NO_2$), VOCs, ammonia (NH_3) and sulfur dioxide (SO_2) that are precursors for O_3, and nitrate and sulfate aerosol formation [*Schultz et al.*, 2008]. Methane (CH_4) is also an important O_3 precursor. Natural wetlands are the dominant single source of CH_4 to the atmosphere. CH_4 is uniquely coupled to O_3, aerosols, and their precursors because the lifetime of this powerful greenhouse gas is controlled by chemical oxidation in the troposphere [*Shindell et al.*, 2009].

Terrestrial ecosystem emissions of trace gas and aerosol precursors are highly sensitive to the vegetation cover and climate state [e.g., *Arneth et al.*, 2010b]. Indeed, altered BVOC emissions have been invoked to

explain CH_4 levels in past hot and cold climates through changed oxidative competition [*Beerling et al.*, 2011; *Valdes et al.*, 2005]. O_3 and aerosols must have been active in Earth's deep past because wildfire and BVOC emissions arose with the evolution of land plants. The warmer and wetter mid-Pliocene climate relative to the preindustrial led to a significantly different vegetation cover [*Salzmann et al.*, 2008]. Paleobotanical data indicate an expansion of tropical savannas and forests at the expense of deserts. Most of the modern arid and semiarid climate zones in Africa, Central Australia, and the Arabian Peninsula were covered with savanna and grassland in the Pliocene. Deciduous forests proliferated, there was a northward shift of temperate and boreal vegetation zones, and grasslands spread on all continents (except Antarctica). Tropical savanna and grassland are highly fire-prone biomes [*Thonicke et al.*, 2010; *van der Werf et al.*, 2010], and deciduous vegetation is a strong isoprene emitter [*Guenther et al.*, 2012]. Therefore, it is likely that the atmospheric composition of O_3 and aerosols was distinctly different in the Pliocene relative to the preindustrial. However, their impact on the Pliocene radiation budget has not previously been assessed, mainly because suitable geochemical or biological proxies do not exist for these chemically reactive, short-lived compounds. In the absence of suitable proxy data, we apply the new generation NASA Goddard Institute for Space Studies Model-E2 global Earth system model [*Schmidt et al.*, 2013] in atmosphere-only configuration forced with boundary conditions from a state-of-the-science paleoenvironmental reconstruction to simulate terrestrial ecosystem emissions and the reactive atmospheric chemical composition in the mid-Pliocene and preindustrial (~1750s) using a time-slab approach. The goal of this study is to provide the first quantitative estimates of the O_3 and aerosol chemistry-climate feedbacks in the mid-Pliocene relative to the preindustrial. We quantify the chemistry-climate feedbacks in terms of the global annual average radiative forcing (RF) metric because it is a good predictor of global average SAT response.

2. Methodology

NASA Model-E2 fully integrates the tropospheric and stratospheric gas-phase chemistry and aerosol modules such that these components interact with each other and with the physics of the climate model [*Shindell et al.*, 2013a]. We use $2° \times 2.5°$ latitude by longitude horizontal resolution with 40 vertical layers extending to 0.1 hPa. The model simulates climate-sensitive terrestrial ecosystem emissions including BVOCs from vegetation [*Unger et al.*, 2013], NO_x from lightning and soils [*Unger et al.*, 2006], and trace gas and aerosol precursors from wildfire activity [*Pechony and Shindell*, 2009, 2010; *Pechony et al.*, 2013]. Further details of the interactive vegetation emission models are provided in the supporting information.

For the mid-Pliocene, the model is forced with boundary conditions (sea surface temperature, sea ice, topography, and vegetation cover) from the Pliocene Research, Interpretation and Synoptic Mapping initiative (PRISM3) data set [*Dowsett et al.*, 2010]. Vegetated land area fractions covered with the major biomes increase significantly from the preindustrial to the mid-Pliocene [*Salzmann et al.*, 2008]: tropical rainforest (13% to 22%), savanna (10% to 17%), grassland (13% to 23%), and deciduous (17% to 24%). Only the evergreen biome has slightly reduced cover in the mid-Pliocene than the preindustrial (10% to 7%). Proxy data from marine geochemical studies suggest that mid-Pliocene CO_2 was in the range 330–400 ppmv [e.g., *Pagani et al.*, 2010; *Raymo et al.*, 1996; *Seki et al.*, 2010]. Proxy reconstructions of mid-Pliocene CH_4 and N_2O are not available, neither is a wetland distribution map. Our strategy is to quantify the atmospheric chemical composition as a function of three plausible mid-Pliocene CH_4 concentrations (1000, 1500, and 2000 ppbv). Warmer and wetter climates likely stimulate N_2O microbial production. On this basis, N_2O radiative forcing is estimated to be about 15% of the sum of the radiative forcing by CO_2 and CH_4 [*Hansen et al.*, 2007].

Preindustrial boundary conditions are approximately representative of the 1750s. Anthropogenic sources of trace gas and aerosol emissions are zero, and atmospheric CO_2, CH_4, and N_2O are prescribed to 280 ppm, 715 ppb, and 275 ppbv, respectively. We apply observed decadal average (1876–1885) monthly varying sea surface temperatures and sea ice from the HadSST2 data set [*Rayner et al.*, 2006]. The vegetation cover is the standard atlas-based distribution in NASA Model-E2 for potential natural vegetation without human land use land cover change.

Integrations of 22 model years are completed for the mid-Pliocene and preindustrial (1750s) simulations; the first 2 years of the simulations are discarded as spin-up, and the remaining 20 years are averaged for analyses. The simulations include the effects of feedbacks from physical climate change on reactive composition but do not allow the online O_3 and aerosol changes to feedback to the radiation and dynamics. We focus on O_3, and carbonaceous, nitrate and sulfate aerosols that have relatively well-constrained direct radiative effects on climate. We do not consider dust, primary biological particles, or aerosol-cloud interactions because the

Table 1. Natural Emissions of O_3 and Aerosol Precursors in the Mid-Pliocene, Preindustrial, and Present Climates[a]

Source/Flux	Mid-Pliocene	Preindustrial	SimA	Present
Vegetation				
Isoprene (TgC/yr)	926	619	782	470
Monoterpene (TgC/yr)	217	251	202	139
GPP (PgC/yr)	195	113	150	124
Wildfire				
NO_x (TgN/yr)	27	14	10	5
CO (Tg/yr)	2429	1160	709	483
Nonmethane VOC (TgC/yr)	35	16	10	7
Black carbon (Tg/yr)	19	9	6	4
Primary organic carbon (Tg/yr)	226	112	75	45
SO_2 (Tg/yr)	20	9	6	4
NH_3 (Tg/yr)	63	30	20	13
Lightning				
NO_x (TgN/yr)	7.6	6.7	6.7	6.7
Soil				
NO_x (TgN/yr)	4.7	3.3	2.5	7.1

[a]SimA is a sensitivity simulation with mid-Pliocene boundary conditions (sea surface temperature, ice sheets, and topography) and preindustrial vegetation cover. The simulated present climate vegetation and wildfire sources agree well with published estimates [*Guenther et al.*, 2012; *Schultz et al.*, 2008; *van der Werf et al.*, 2010].

radiative impacts of these processes are less certain, and the sign (net warming or cooling) is not robust across models. The difference between the mid-Pliocene and preindustrial time-slice simulations allows us to isolate the RF due to O_3 and multiple aerosol species (black carbon, primary organic matter, BSOA, sulfate, and nitrate) [*Unger et al.*, 2010]. The long-lived greenhouse gas RFs are determined using analytic expressions based on the known and/or assumed atmospheric concentration changes [*Forster et al.*, 2007]. To assess the relative roles of physical climate (temperature and precipitation) versus vegetation cover on the terrestrial ecosystem emissions, we perform an additional sensitivity simulation that applies the mid-Pliocene boundary conditions but is forced with preindustrial vegetation cover (SimA).

3. Results

3.1. Terrestrial Ecosystem Emissions in the Mid-Pliocene and Preindustrial

Simulated mid-Pliocene minus preindustrial global average SAT and precipitation changes are +2.4°C and 0.16 mm/day (Figure S1a). Increased greenhouse gas concentrations in the warmer climate drive temperature increases throughout the troposphere and temperature decreases in the stratosphere (Figure S1b). Using the PRISM3 boundary conditions, the model reproduces the polar amplification of warming and marked increase in precipitation over tropical continents. The model simulates substantially higher terrestrial ecosystem emissions of O_3 and aerosol precursors in the mid-Pliocene relative to the preindustrial (Table 1). Gross primary productivity in the mid-Pliocene is about double the preindustrial value (195 versus 113 Pg C/yr). Based on SimA results, about half of the increase is due to the vegetation cover change and the other half is due to the warmer, wetter, high-CO_2 ancient climate. Our results suggest a more active land carbon cycle in the mid-Pliocene than the preindustrial, which may partly contribute to the higher steady state atmospheric CO_2 level. The mid-Pliocene global isoprene source is 50% higher than the preindustrial value. Similar to GPP, about half of the higher mid-Pliocene isoprene source relative to the preindustrial can be attributed to the vegetation cover change, in particular the increase in deciduous and tropical rainforest biome cover (Figure S2a). In contrast, global monoterpene emission is slightly lower in the mid-Pliocene than preindustrial. The major monoterpene emission region shifts northward in the mid-Pliocene relative to the preindustrial following the poleward shift in the evergreen biome (Figure S2b).

Preindustrial wildfire emissions are approximately double present-day estimates obtained using the same model (Table 1), which is consistent with data from historical ice core and continuous sedimentary charcoal records [*Marlon et al.*, 2008; *Power et al.*, 2008; *van der Werf et al.*, 2013]. The full reasons are not completely understood but are likely related to increased fuel loading and lack of human fire suppression. The model suggests a further doubling of wildfire emissions in the mid-Pliocene over preindustrial estimates. Similarly, wildfire activity has been projected to increase in the future, warmer world [*Yue et al.*, 2013]. In the model, the

mid-Pliocene increase is driven entirely by the vegetation cover change, specifically the spread of tropical savanna (Figures S2c and S2d). The mid-Pliocene physical climate conditions, especially humidity and precipitation, actually act to suppress the fire activity relative to the preindustrial (Table 1, SimA). Globally, on centennial to millennial timescales, temperature is the major driver of changes in wildfire activity: Increasing temperature leads to increased fire through increasing plant productivity and hence fuel production [*Bowman et al*., 2009]. The effect of precipitation on wildfire is more complex. Fire peaks at intermediate precipitation levels at all temperatures: Fire is low in dry environments because of lack of fuel and in wet environments because the fuel is too damp to burn.

Records of macroscopic charcoal can be used to track wildfire in Earth's history [*Bowman et al*., 2009; *Scott*, 2000]. While it is not possible to derive a quantitative comparison of relative fire activity between the mid-Pliocene and preindustrial because continuous charcoal records extend back only about 320K years, a dramatic increase in charcoal occurrence in deep marine sediments over the past ~7 Ma has been found [*Bond and Scott*, 2010; *Herring*, 1985]. The increase coincides with the spread of tropical savanna and grassland in the late Cenozoic. The most likely explanation for the increased charcoal flux into the late Cenozoic sediments appears to be due to increased plant burning on land, especially tropical savanna burning and the coupled fire-grass system [*Bond and Keeley*, 2005; *Osborne and Beerling*, 2006].

3.2. Chemical Forcing of Mid-Pliocene Climate

The mid-Pliocene increases in terrestrial ecosystem emissions act to increase the atmospheric loading of O_3 and aerosols relative to the preindustrial (Table S1 and Figure S3). The increases in wildfire emissions drive a doubling of the black carbon and primary organic matter aerosol burdens (Table S1). The vegetation BVOC emission increases lead to a 40% increase in BSOA burden. In addition, nitrate aerosol burden increases by about 20%, and sulfate decreases by about 10% (although its atmospheric level is almost negligible compared to other particle types in the Pliocene). The substantial increases in BSOA and nitrate in the mid-Pliocene parallel previous findings that these aerosol types will play an increasingly important role in a future warmer, low sulfur emission world [*Bellouin et al*., 2011; *Kulmala et al*., 2004].

Compared to the preindustrial, the O_3 burden is ~25% higher in the troposphere and ~5% higher in the stratosphere. The enhanced Pliocene stratospheric O_3 burden is a result of increased tropical upwelling, and colder stratospheric temperatures in the warmer climate state (Figure S1b), which slow the gas-phase chemical reactions that destroy O_3 [*Waugh et al*., 2009]. An important consequence is ~20% lower tropospheric $J(O^1D)$ photolysis rate, which reduces the primary production of the major tropospheric oxidant, the hydroxyl radical (OH) (Table S1 and Figure S3). The mid-Pliocene CO burden doubles, while the NO_x burden is similar to the preindustrial value, indicating a relative increase in the OH sink. Overall, zonal average mass-weighted tropospheric OH is 20–25% lower resulting in a 20–30% (3–4 years) longer CH_4 lifetime than in the preindustrial world. Remarkably, the preindustrial to Pliocene paleoclimate change represents a positive feedback on the climate system through CH_4, in contrast to the (albeit much smaller) preindustrial to present-day anthropogenic climate change that represents a negative feedback through CH_4 [*Naik et al*., 2013]. Comparison of the preindustrial composition model output against limited data available from ice cores suggests that the 1750s simulation is reasonable (supporting information).

The mid-Pliocene changes in O_3 and aerosol composition alter Earth's radiation balance. The CO_2 RF (based on 330–400 minus 280 ppmv) is $+1.29 \pm 0.52$ Wm^{-2}. The chemistry-climate feedbacks contribute both warming and cooling effects (Figure 1 and Table S2) and are of strikingly similar magnitude to anthropogenic O_3 and aerosol RFs caused by increases in fossil fuel and biofuel burning [e.g., *Forster et al*., 2007]. Total aerosol direct cooling effects are about -0.71 Wm^{-2}, masking 15–100% of the CO_2 RF, and are independent of the CH_4 level. The combined warming chemistry-climate feedbacks may enhance the CO_2 RF by +30–250% depending on CH_4 level. Our estimates of the net RF for each CH_4 scenario (1000, 1500, and 2000 ppbv) including all components (CO_2 + non-CO_2) are (in Wm^{-2}) $+1.48 \pm 0.81$, 1.78 ± 0.83, and 2.03 ± 0.85. The net positive chemistry-climate feedbacks support a higher mid-Pliocene global average SAT than has been obtained with the known external forcings from CO_2 and surface albedo changes.

The O_3 and aerosols cause a markedly heterogeneous spatial distribution in the net RF (Figures 1 and S4). In the tropics, the local chemistry-climate contributions to RF are an order of magnitude larger than the CO_2 RF. The effects of primary organic matter and BSOA combine to yield a net negative RF up to -15 Wm^{-2} over the

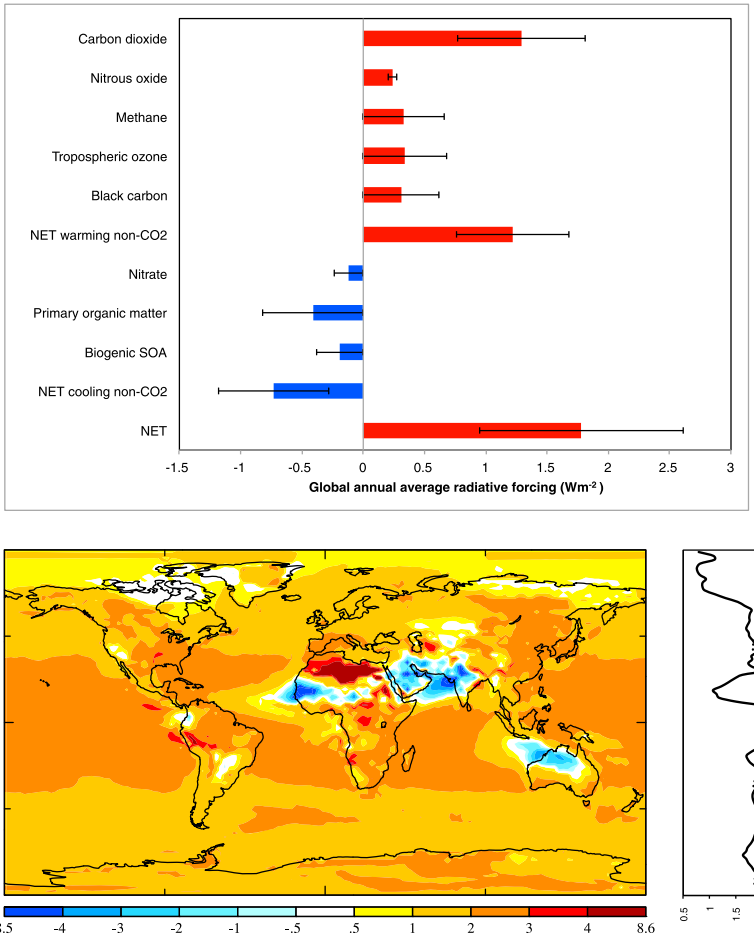

Figure 1. (top) Mid-Pliocene minus preindustrial chemical forcing of climate by component (results shown for the CH_4 = 1500 ppbv case). The uncertainty assessment and the results for all CH_4 cases are detailed in Table S2. (bottom) Spatial distribution of net sum of all RF components above. Units are Wm^{-2} (individual short-lived climate forcing components are shown in Figure S4). Zonal average net RF is shown in Figure 1 (bottom, right) for the mid-Pliocene minus preindustrial ~1750s (solid line) and a representative sample for the anthropogenic present day minus preindustrial ~1850 s (dotted line) [e.g., *Shindell et al.*, 2013b].

tropical and subtropical savanna and grassland biomes in Africa, the Middle East, and Australia. In North Africa, the warming black carbon and O_3 effects yield a strong local positive forcing up to +10 Wm^{-2}. The mid-Pliocene minus preindustrial net RF displays an unusual equator to pole gradient compared to anthropogenic present-day minus preindustrial net RF (Figure 1). For instance, the mid-Pliocene minus preindustrial net RF in the Northern Hemisphere has a minimum in the subtropics and polar region and maximum in the midlatitudes. Quantifying the relationship between regionally distributed RFs and regional climate response is a newly emerging research area [*Fiore et al.*, 2012]. We propose that the spatial distribution of net RF caused by the chemistry-climate feedbacks offers a new alternative mechanism to explain some of the structural differences in Pliocene climate relative to the preindustrial. We will test this hypothesis in future work using a version of the model with a fully coupled dynamic ocean. In turn, allowing the atmospheric chemistry to influence the climate system dynamics may alter the strength of the feedback itself.

4. Discussion and Conclusions

We have discovered large O_3 and non-dust aerosol radiative perturbations caused by increases in terrestrial ecosystem emissions in the warmer and wetter ancient climate of the mid-Pliocene. The altered vegetation cover between the mid-Pliocene and the preindustrial is the dominant driver of the emission changes and therefore the radiative impacts. Vigorous atmospheric chemistry played an important role in past warm climates and is not a human-made phenomenon.

There are several limitations to the present study. We concede large uncertainties in the magnitude and regional variability of wildfire activity and emissions [*Schultz et al*., 2008]. Prognostic modeling of terrestrial ecosystem emissions is still in early research phases. Furthermore, the Pliocene chemistry-climate feedbacks newly identified in this work depend on the PRISM3 boundary conditions for which considerable uncertainties exist. The vegetation cover reconstruction uses paleobotanical data from across the entire 1 million year period between 3.6–2.6 Ma and selects the vegetation data that represents the warmest climatic conditions even though significant variability occurred during this period [*Haywood et al*., 2013]. We postulate that the Pliocene chemistry-climate feedbacks are not strongly sensitive to biases in the vegetation reconstruction because the least stable biomes (the Arctic and western North America) are not important sources of the terrestrial ecosystem emissions that drive our results [*Salzmann et al*., 2013]. However, it is likely that the Pliocene chemistry-climate feedbacks are sensitive to the known Northern Hemisphere surface temperature cold bias in current generation climate models [*Salzmann et al*., 2013]. We speculate that this discrepancy implies an underestimation of the strength of the chemistry-climate interactions here because the terrestrial ecosystem emissions have a positive temperature dependence.

In all paleoclimate sensitivity studies to date, O_3 and aerosols have been dismissed as fast feedbacks on the basis that their transport and chemistry are sensitive to meteorology such that in warmer and wetter climate states their atmospheric lifetimes would be shorter [*Rohling et al*., 2012]. Our findings seriously challenge this assumption and are consistent with assessments of high Earth system climate sensitivity for the Pliocene [*Lunt et al*., 2010; *Pagani et al*., 2010]. This discovery has implications for all prehuman climate states and for understanding the climate impacts of human land use.

Acknowledgments

Funding for this research is provided by Yale University. The authors thank L. Sohl, M. Chandler, and the NASA GISS Model-E2 development team. The authors are grateful to A. Scott and J. Marlon for helpful discussions. This project was supported in part by the facilities and staff of the Yale University Faculty of Arts and Sciences High Performance Computing Center.

The Editor thanks Alan Haywood and an anonymous reviewer for their assistance in evaluating this paper.

References

Arneth, A., et al. (2010a), From biota to chemistry and climate: Towards a comprehensive description of trace gas exchange between the biosphere and atmosphere, *Biogeosciences*, *7*(1), 121–149.

Arneth, A., et al. (2010b), Terrestrial biogeochemical feedbacks in the climate system, *Nat. Geosci.*, *3*(8), 525–532.

Ballantyne, A. P., D. R. Greenwood, J. S. S. Damste, A. Z. Csank, J. J. Eberle, and N. Rybczynski (2010), Significantly warmer Arctic surface temperatures during the Pliocene indicated by multiple independent proxies, *Geology*, *38*(7), 603–606.

Beerling, D. J., A. Fox, D. S. Stevenson, and P. J. Valdes (2011), Enhanced chemistry-climate feedbacks in past greenhouse worlds, *Proc. Natl. Acad. Sci. U.S.A.*, *108*(24), 9770–9775.

Bellouin, N., J. Rae, A. Jones, C. Johnson, J. Haywood, and O. Boucher (2011), Aerosol forcing in the Climate Model Intercomparison Project (CMIP5) simulations by HadGEM2-ES and the role of ammonium nitrate, *J. Geophys. Res.*, *116*, D20206, doi:10.1029/2011JD016074.

Bond, W. J., and A. C. Scott (2010), Fire and the spread of flowering plants in the Cretaceous, *New Phytol.*, *188*(4), 1137–1150.

Bond, W. J., and J. E. Keeley (2005), Fire as a global "herbivore": The ecology and evolution of flammable ecosystems, *Trends Ecol. Evol.*, *20*(7), 387–394.

Bowman, D. M. J. S., et al. (2009), Fire in the Earth system, *Science*, *324*(5926), 481–484.

Carslaw, K. S., O. Boucher, D. V. Spracklen, G. W. Mann, J. G. L. Rae, S. Woodward, and M. Kulmala (2010), A review of natural aerosol interactions and feedbacks within the Earth system, *Atmos. Chem. Phys.*, *10*(4), 1701–1737.

Dowsett, H. J., M. Robinson, A. Haywood, U. Salzmann, D. Hill, L. Sohl, M. Chandler, M. Williams, K. Foley, and D. Stoll (2010), The PRISM3D paleoenvironmental reconstruction, *Stratigraphy*, *7*(2–3), 123–139.

Dowsett, H. J., et al. (2012), Assessing confidence in Pliocene sea surface temperatures to evaluate predictive models, *Nat. Clim. Change*, *2*(5), 365–371.

Fedorov, A. V., C. M. Brierley, K. T. Lawrence, Z. Liu, P. S. Dekens, and A. C. Ravelo (2013), Patterns and mechanisms of early Pliocene warmth, *Nature*, *496*(7443), 43–49.

Fiore, A. M., et al. (2012), Global air quality and climate, *Chem. Soc. Rev.*, *41*(19), 6663–6683.

Forster, P., et al. (2007), Changes in atmospheric constituents and in radiative forcing, in *Climate Change 2007: The Physical Science Basis. Contribution of Working Group I to the Fourth Assessment Report of the Intergovernmental Panel on Climate Change*, edited by S. Solomon et al., pp. 129–234, Cambridge Univ. Press, Cambridge, U.K.

Guenther, A. B., X. Jiang, C. L. Heald, T. Sakulyanontvittaya, T. Duhl, L. K. Emmons, and X. Wang (2012), The Model of Emissions of Gases and Aerosols from Nature version 2.1 (MEGAN2.1): An extended and updated framework for modeling biogenic emissions, *Geosci. Model. Dev.*, *5*(6), 1471–1492.

Hansen, J., M. Sato, P. Kharecha, G. Russell, D. W. Lea, and M. Siddall (2007), Climate change and trace gases, *Philos. Trans. R. Soc. A*, *365*(1856), 1925–1954.

Haywood, A. M., and P. J. Valdes (2004), Modelling Pliocene warmth: Contribution of atmosphere, oceans and cryosphere, *Earth Planet Sci. Lett.*, *218*(3–4), 363–377.

Haywood, A. M., et al. (2010), Pliocene Model Intercomparison Project (PlioMIP): Experimental design and boundary conditions (Experiment 1), *Geosci. Model. Dev.*, *3*(1), 227–242.

Haywood, A. M., et al. (2013), On the identification of a pliocene time slice for data-model comparison, *Philos. Trans. R. Soc. A*, *371*(2001), 1471–2962.

Herring, J. R. (1985), Charcoal fluxes into sediments of the North Pacific Ocean: The Cenozoic record of burning, *Geophys. Monogr. Ser.*, *32*, 419–442.

Kulmala, M., et al. (2004), A new feedback mechanism linking forests, aerosols, and climate, *Atmos. Chem. Phys.*, *4*, 557–562.

Lunt, D. J., A. M. Haywood, G. A. Schmidt, U. Salzmann, P. J. Valdes, and H. J. Dowsett (2010), Earth system sensitivity inferred from Pliocene modelling and data, *Nat. Geosci.*, *3*(1), 60–64.

Marlon, J. R., P. J. Bartlein, C. Carcaillet, D. G. Gavin, S. P. Harrison, P. E. Higuera, F. Joos, M. J. Power, and I. C. Prentice (2008), Climate and human influences on global biomass burning over the past two millennia, *Nat. Geosci.*, *1*(10), 697–702.

Naik, V., et al. (2013), Preindustrial to present-day changes in tropospheric hydroxyl radical and methane lifetime from the Atmospheric Chemistry and Climate Model Intercomparison Project (ACCMIP), *Atmos. Chem. Phys.*, *13*(10), 5277–5298.

Osborne, C. P., and D. J. Beerling (2006), Nature's green revolution: The remarkable evolutionary rise of C-4 plants, *Philos. Trans. R. Soc. B*, *361*(1465), 173–194.

Pagani, M., Z. H. Liu, J. LaRiviere, and A. C. Ravelo (2010), High Earth-system climate sensitivity determined from Pliocene carbon dioxide concentrations, *Nat. Geosci.*, *3*(1), 27–30.

Pechony, O., and D. T. Shindell (2009), Fire parameterization on a global scale, *J. Geophys. Res.*, *114*, D16115, doi:10.1029/2009JD011927.

Pechony, O., and D. T. Shindell (2010), Driving forces of global wildfires over the past millennium and the forthcoming century, *Proc. Natl. Acad. Sci. U.S.A.*, *107*(45), 19,167–19,170.

Pechony, O., D. T. Shindell, and G. Faluvegi (2013), Direct top-down estimates of biomass burning CO emissions using TES and MOPITT versus bottom-up GFED inventory, *J. Geophys. Res. Atmos*, *118*, 1–13, doi:10.1002/jgrd.50624.

Power, M. J., et al. (2008), Changes in fire regimes since the Last Glacial Maximum: An assessment based on a global synthesis and analysis of charcoal data, *Clim. Dyn.*, *30*(7–8), 887–907.

Raymo, M. E., B. Grant, M. Horowitz, and G. H. Rau (1996), Mid-Pliocene warmth: Stronger greenhouse and stronger conveyor, *Mar. Micropaleontol.*, *27*(1–4), 313–326.

Rayner, N. A., P. Brohan, D. E. Parker, C. K. Folland, J. J. Kennedy, M. Vanicek, T. J. Ansell, and S. F. B. Tett (2006), Improved analyses of changes and uncertainties in sea surface temperature measured in situ sice the mid-nineteenth century: The HadSST2 dataset, *J. Clim.*, *19*(3), 446–469.

Robinson, M. M. (2009), New quantitative evidence of extreme warmth in the Pliocene Arctic, *Stratigraphy*, *6*(4), 265–275.

Rohling, E. J., et al. (2012), Making sense of palaeoclimate sensitivity, *Nature*, *491*(7426), 683–691.

Salzmann, U., A. M. Haywood, D. J. Lunt, P. J. Valdes, and D. J. Hill (2008), A new global biome reconstruction and data-model comparison for the Middle Pliocene, *Global Ecol. Biogeogr.*, *17*(3), 432–447.

Salzmann, U., et al. (2013), Challenges in quantifying Pliocene terrestrial warming revealed by data-model discord, *Nat. Clim. Change*, *3*(11), 969–974.

Schmidt, G. A., et al. (2013), Configuration and assessment of the GISS ModelE2 contributions to the CMIP5 archive, *J. Adv. Model. Earth Syst.*, in press.

Schultz, M. G., A. Heil, J. J. Hoelzemann, A. Spessa, K. Thonicke, J. G. Goldammer, A. C. Held, J. M. C. Pereira, and M. van het Bolscher (2008), Global wildland fire emissions from 1960 to 2000, *Global Biogeochem. Cycle*, *22*, GB2002, doi:10.1029/2007GB003031.

Scott, A. C. (2000), The Pre-Quaternary history of fire, *Palaeogeogr. Palaeoclimatol. Palaeoecol.*, *164*(1–4), 281–329.

Seki, O., G. L. Foster, D. N. Schmidt, A. Mackensen, K. Kawamura, and R. D. Pancost (2010), Alkenone and boron-based Pliocene pCO(2) records, *Earth Planet Sci. Lett.*, *292*(1–2), 201–211.

Shindell, D. T., G. Faluvegi, D. M. Koch, G. A. Schmidt, N. Unger, and S. E. Bauer (2009), Improved attribution of climate forcing to emissions, *Science*, *326*(5953), 716–718.

Shindell, D. T., et al. (2013a), Interactive ozone and methane chemistry in GISS-E2 historical and future climate simulations, *Atmos. Chem. Phys.*, *13*(5), 2653–2689.

Shindell, D. T., et al. (2013b), Radiative forcing in the ACCMIP historical and future climate simulations, *Atmos. Chem. Phys.*, *13*(5), 2939–2974.

Thonicke, K., A. Spessa, I. C. Prentice, S. P. Harrison, L. Dong, and C. Carmona-Moreno (2010), The influence of vegetation, fire spread and fire behaviour on biomass burning and trace gas emissions: Results from a process-based model, *Biogeosciences*, *7*(6), 1991–2011.

Unger, N., D. T. Shindell, D. M. Koch, M. Amann, J. Cofala, and D. G. Streets (2006), Influences of man-made emissions and climate changes on tropospheric ozone, methane, and sulfate at 2030 from a broad range of possible futures, *J. Geophys. Res.*, *111*, D12313, doi:10.1029/2005JD006518.

Unger, N., T. C. Bond, J. S. Wang, D. M. Koch, S. Menon, D. T. Shindell, and S. Bauer (2010), Attribution of climate forcing to economic sectors, *Proc. Natl. Acad. Sci. U.S.A.*, *107*(8), 3382–3387.

Unger, N., et al. (2013), Photosynthesis-dependent isoprene emission from leaf to planet in a global carbon-chemistry-climate model, *Atmos. Chem. Phys.*, *13*, 10,243–10,269.

Valdes, P. J., D. J. Beerling, and C. E. Johnson (2005), The ice age methane budget, *Geophys. Res. Lett.*, *32*, L02704, doi:10.1029/2004GL021004.

van der Werf, G. R., J. T. Randerson, L. Giglio, G. J. Collatz, M. Mu, P. S. Kasibhatla, D. C. Morton, R. S. DeFries, Y. Jin, and T. T. van Leeuwen (2010), Global fire emissions and the contribution of deforestation, savanna, forest, agricultural, and peat fires (1997–2009), *Atmos. Chem. Phys.*, *10*(23), 11,707–11,735.

van der Werf, G. R., W. Peters, T. T. van Leeuwen, and L. Giglio (2013), What could have caused pre-industrial biomass burning emissions to exceed current rates?, *Clim. Past*, *9*(1), 289–306.

Waugh, D. W., L. Oman, S. R. Kawa, R. S. Stolarski, S. Pawson, A. R. Douglass, P. A. Newman, and J. E. Nielsen (2009), Impacts of climate change on stratospheric ozone recovery, *Geophys. Res. Lett.*, *36*, L03805, doi:10.1029/2008GL036223.

Yue, X., L. J. Mickley, J. A. Logan, and J. O. Kaplan (2013), Ensemble projections of wildfire activity and carbonaceous aerosol concentrations over the western United States in the mid-21st century, *Atmos. Environ.*, *77*, 767–780.